A Unified View of Computational Electromagnetics

Zhizhang Chen, *Fellow, IEEE*, Chao-Fu Wang, *Senior Member, IEEE*, and Wolfgang J. R. Hoefer, *Life Fellow, IEEE*

(Invited Paper)

***Abstract*— This article presents a unified description of numerical methods for solving electromagnetic field problems. Traditionally, these methods are considered to be independent and alternative ways of solving Maxwell's equations or equations derived therefrom. However, they all are projective approximations of the unknown solution by known expansion or basis functions with unknown amplitude coefficients that are determined using the so-called method of weighted residuals (MWR). This common feature forms the proposed unifying framework that may serve both as a systematic introduction to computational electromagnetics and as a way to provide insight into the nature, strengths, and limitations of the various algorithms used by present and future field solvers. For convenience, the fundamental equations and concepts of electromagnetics are summarized in order to facilitate the demonstration of the unified approach. Our aim is to provide students, designers, and researchers with a framework for developing new numerical algorithms, to guide users in the selection and application of electromagnetic design tools, and to foster informed engineering judgment. This article also serves as a review and summary of earlier theoretical works reported in different places and at different times.**

***Index Terms*— Basis function, expansion, inner product, method of moments (MoM), method of weighted residuals (MWR), projective approximation, unification, weighting function.**

I. Introduction

THE existential challenges of the natural world have compelled humans to explore the laws that govern its structure and its evolution. This endeavor is not only motivated by curiosity but also by the need to survive and the desire to harness the forces of nature. It is a two-pronged effort: one aims to *comprehend* the physical world as it is: the natural sciences and their mathematical and experimental frameworks aim to understand nature and to predict the outcome of certain actions and events. The other leverages the sciences, mathematics, and experimentation to create new objects, systems, and processes that do not exist in nature through engineering design.

In all these activities, the key to success is the ability to model the essential physical processes as accurately as possible. A model can be conceptual, physical, mathematical, or computational; the latter has emerged as the dominant, most versatile, and powerful tool in modern engineering analysis and design by virtue of digital computers. In electrical and computer engineering, including microwave, millimeter-wave, high-speed electronics, and computers, electromagnetic fields are utilized to transmit and process information and power, and they are fundamentally governed by Maxwell's equations. Though there are other tools to solve Maxwell's equations, numerical modeling is the most versatile, effective way, resulting in electromagnetic simulators or field solvers. Without the field solvers, the evolution of analog and digital systems toward ever higher clock rates, higher frequencies, larger bandwidths, higher packaging density, and higher complexity would be inconceivable. The ability to accurately model a complete electromagnetic system is indispensable for rapid product development, short time to market, and conformity with susceptibility and emission standards.

This article will focus on the prevalent computational models for solving electromagnetic problems. Its scope is to present the existing methods, not in the traditional way as a collection of distinct, unrelated paradigms, but rather as a set of related methods with common central features yet possessing individual properties suitable for solving a diverse range of problems. It is hoped that this unified approach will serve both as a systematic introduction to computational methods in electromagnetics and as a way to provide insight into the nature, strengths, and limitations of the algorithms used by present and future field solvers, guide the selection and application of electromagnetic design tools, develop new numerical algorithms, and foster informed engineering judgment. Moreover, this article can serve as a collocating review and summary of earlier works reported previously.

A. Computational Electromagnetics

The theory and practice of solving electromagnetic field problems on digital computers are known as computational or numerical electromagnetics. Its purpose is to find solutions

Manuscript received July 19, 2021; revised September 12, 2021; accepted December 5, 2021. Date of publication January 14, 2022; date of current version February 7, 2022. This work was supported in part by the Natural Science and Engineering Research Council of Canada through its Discovery Grant Program, Fuzhou University, through its Internal Research Program; and in part by the Natural Science Foundation of China through its General under Grant 62071125. *(Corresponding author: Zhizhang Chen.)*

Zhizhang Chen is with the College of Physics and Information Engineering, Fuzhou University, Fuzhou, Fujian 350108, on leave from the Department of Electrical and Computer Engineering, Dalhousie University, Halifax, NS B3H 4R2, Canada (e-mail: zz.chen@ieee.org).

Chao-Fu Wang is with the Department of Electrical and Computer Engineering, National University of Singapore, Singapore 117411 (e-mail: cfwang@nus.edu.sg).

Wolfgang J. R. Hoefer is with the Department of Electrical and Computer Engineering, University of Victoria, Victoria, BC V8S 2N3, Canada (e-mail: wolfgang@wolfganghoefer.com).

Color versions of one or more figures in this article are available at https://doi.org/10.1109/TMTT.2021.3138911.

Digital Object Identifier 10.1109/TMTT.2021.3138911

to Maxwell's equations or equations derived from them that satisfy all boundary and interface conditions, electromagnetic properties of materials, and excitation conditions specified in a given problem. All computational models are discretized and thus yield only *approximate* solutions of Maxwell's equations, except in some special cases. Their accuracy depends on several factors and usually converges with increasing computational expenditure. The convergence of a particular numerical method is important when assessing the validity of simulation results and will thus be addressed in this article.

B. Maxwell's Equations and Equations Derived From Them

The first model of electromagnetic fields was developed by Maxwell [1] over 150 years ago, restated in its present form by Heaviside [2], and experimentally validated by Hertz [3]. It is a purely mathematical model that has stood the test of time. Unlike most other laws of classical physics, it requires no relativistic correction since the concept of magnetic force accounts for the relativistic change of the electric force between moving charges. However, it breaks down at the atomic scale, where the laws of quantum electromagnetics prevail [4], [5].

Maxwell's equations thus continue to be the foundation of mainstream electrical and electronic engineering and computer technology. They can be written in the well-known differential form and are shown here for convenience [2]

$$\begin{cases} \nabla \times \mathbf{E} = -\dfrac{\partial \mathbf{B}}{\partial t} \\ \nabla \times \mathbf{H} = \dfrac{\partial \mathbf{D}}{\partial t} + \mathbf{J} \\ \nabla \cdot \mathbf{D} = \rho \\ \nabla \cdot \mathbf{B} = 0. \end{cases} \tag{1}$$

While (1) is the set of the original electromagnetic field equations, there exist other equations derived from (1). One of the most well-known is the wave equation [6]

$$\begin{cases} \nabla^2 \mathbf{E} - \dfrac{1}{c^2}\dfrac{\partial^2 \mathbf{E}}{\partial t^2} = \dfrac{\nabla \rho}{\varepsilon} + \mu \dfrac{\partial \mathbf{J}}{\partial t} \\ \nabla^2 \mathbf{H} - \dfrac{1}{c^2}\dfrac{\partial^2 \mathbf{H}}{\partial t^2} = -\mu \nabla \times \mathbf{J} \end{cases} \tag{2}$$

where ε and μ are the permittivity and permeability of solution domain, respectively, $c = 1/(\mu\varepsilon)^{1/2}$ is the constant speed of light, and ∇ is the *del* operator (or *Nabla* operator). Another well-known equation derived from (1) in the static limit of putting all derivatives with respect to time to zero is Poisson's equation for the scalar electric potential φ (as a function of the charge density distribution ρ)

$$\nabla^2 \varphi = -\frac{\rho}{\varepsilon}, \text{ where } \nabla \varphi = -\mathbf{E} \tag{3}$$

which becomes Laplace's equation when $\rho = 0$. Solutions of (2) are also solutions of Maxwell's equations, and (2) can thus serve as the basis for a specialized computational algorithm.

Whatever electromagnetic equation we choose as a starting point for a computational model, the resulting numerical method can be interpreted mathematically as a *projective approximation* to the exact solution of Maxwell's equations, a concept for solving differential and integral equations (IEs) that is backed by an extensive mathematical framework developed since the early 1900s [7]–[9]. The literature on this subject is extensive. We can summarize here only the essential concepts and ideas while referring the reader to the list of specialized works on the various numerical techniques in the bibliography (e.g., [10]).

C. Projective Approximation of Electromagnetic Solutions

The solutions of Maxwell's equations are functions of space and either time or frequency (see Section II). Their projective representation is performed in function space, also called "inner product space," an abstract concept that is best understood by analogy to the projection of a vector upon the coordinates of Euclidian space [11], [12]. A function space is spanned by known basis or expansion functions with unknown coefficients. The solution strategy is to find the values of these coefficients such that their resultant linear combination or expansion approximates the exact solution as closely as possible. This strategy is known as the method of weighted residuals (MWR) and is the subject of Section III: it shows that a computational model is a projective approximation in the inner product space of the solution of an operator equation. Section IV presents a unified view of the formulation of numerical methods in terms of the MWR. Finally, Section V summarizes and concludes the article.

II. Solution Domains

Electromagnetic phenomena occur naturally in space and time. The original Maxwell equations (1) and (2) are formulated in the time domain, and their solutions are functions of space and time as well. However, it is more convenient to project and solve an electromagnetic problem in a different domain in many situations, such as the frequency domain or the spectral domain. Since they are fundamental to this article, they will be recalled here before entering the main subject.

A. Time Domain

Humans experience events and processes in the time domain. There are several definitions of time. One which we consider most relevant to this article is time as a continuous, measurable quantity in which events occur in a sequence progressing from the past through the present to the future. In theory, the time domain ranges from an infinite past to an infinite future. Mathematically, it is represented as $-\infty \leq t \leq +\infty$ or $t \in [-\infty, +\infty]$. A finite time interval between t_1 and t_2 is more realistic, i.e., $t_1 \leq t \leq t_2$ or $t \in [t_1, t_2]$. Note that in the real universe, time always evolves from the past to the future, while in mathematical and computational models, time can flow from the future to the past, which is known as computational time reversal [13] and is part of the so-called inverse methods [14].

B. Frequency Domain

A frequently used signal or function that is easy to generate by electronic hardware is the time-harmonic signal of the form

$$g_s(t) = A_s \cos(\omega t + \varphi_s). \tag{4}$$

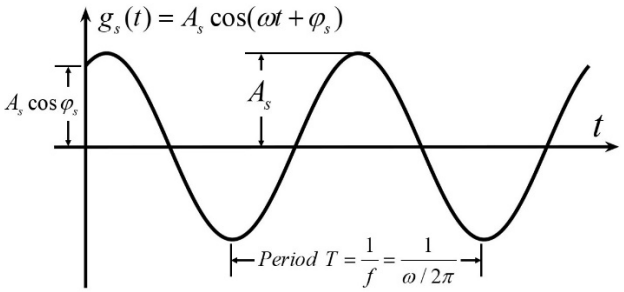

Fig. 1. Graphical illustration of a time-harmonic or sinusoidal signal.

Three parameters define a sinusoidal signal (see Fig. 1): the amplitude A_s, the angular frequency $\omega = 2\pi f$, and the phase φ_s (which determines the initial value of the signal). Equation (5) can also be mathematically represented by a complex number, often called phasor

$$g_s(t) = \mathrm{Re}\left[A_s e^{j(\omega t+\varphi_s)}\right] = \mathrm{Re}\left[\underbrace{A_s e^{j\varphi_s}}_{\text{Phasor}} e^{j\omega t}\right] = \mathrm{Re}\left[\underbrace{G_s}_{\text{phasor}} e^{j\omega t}\right] \tag{5}$$

where the phasor $G_s = A_s e^{j\varphi_s}$ is a complex number, its magnitude being the amplitude and the phase being the phase of the sinusoidal signal.

Fourier has shown that a signal or a function of time $g(t)$ can be considered as a sum of many sinusoidal signals of different frequencies like (4). The phasors of these sinusoidal signals are obtained through the well-known Fourier transform [15]

$$G(\omega) = \mathcal{F}[g(t)] = \int_{-\infty}^{+\infty} g(t)e^{-j\omega t}dt. \tag{6}$$

It yields the amplitude and phase of the sinusoidal signal component of $g(t)$ at a specific angular frequency ω or a specific temporal frequency $f = \omega/2\pi$, respectively.

Once $G(\omega)$ is known (sometimes through measurements), the original time-domain signal $g(t)$ can be obtained through the so-called Inverse Fourier transform

$$g(t) = \mathcal{F}^{-1}[G(\omega)] = \frac{1}{2\pi}\int_{-\infty}^{+\infty} G(\omega)e^{+j\omega t}d\omega. \tag{7}$$

Note that the upper integration limit is $+\infty$ and the lower integration limit $-\infty$. It means that $G(\omega)$ of the entire frequency spectrum needs to be known in theory to obtain the corresponding time function.

The Fourier transform has many operational properties. The most often used in computational electromagnetics are the differential and integral operations

$$\mathcal{F}\left[\frac{d^n g(t)}{dt^n}\right] = (j\omega)^n \mathcal{F}[g(t)] = (j\omega)^n G(\omega) \tag{8}$$

$$\mathcal{F}\left[\int_{-\infty}^{t} g(\tau)d\tau\right] = \frac{G(\omega)}{j\omega} + \frac{1}{2}G(0)\delta(\omega). \tag{9}$$

They basically state that a time derivative is equivalent to a multiplication by $j\omega$, and time integration is equivalent to a division by $j\omega$ in the frequency domain. For further information on the Fourier transform, readers are referred to the excellent book by Poularikas [15].

With the Fourier transform, electromagnetic problems can be solved in the so-called frequency domain. Specifically, we apply Fourier transform to the original Maxwell's equations or their derived equations, and the resulting equations are then the corresponding frequency-domain equations. For instance, (2) becomes

$$\begin{cases} \nabla^2\mathbf{E} + \left(\dfrac{\omega}{c}\right)^2\mathbf{E} = \dfrac{\nabla\rho}{\varepsilon} + j\omega\mu\mathbf{J} \\ \nabla^2\mathbf{H} + \left(\dfrac{\omega}{c}\right)^2\mathbf{H} = -\mu\nabla\times\mathbf{J}. \end{cases} \tag{10}$$

Equations (10) are called the Helmholtz equations. The differential operations in time in (1) and (2) are now replaced by simple arithmetic multiplication by $j\omega$, reducing the problem complexity by one dimension.

On the other hand, the electromagnetic solutions to (10) are valid at a specific frequency f or angular frequency $\omega = 2\pi f$. They represent the magnitude and the phase of electromagnetic fields at that frequency. Such solutions are the so-called frequency-domain solutions. To recover the original time-domain electromagnetic fields or signals, we need to know the frequency-domain solutions over the entire frequency domain of $\omega \in [-\infty, +\infty]$ or $f \in [-\infty, +\infty]$ through either computations or measurements so that we can apply the inverse Fourier transform given in (7).

C. Spectral Domain

In Section II-B, we take the Fourier transform with respect to time, i.e., we perform the integration with respect to time t in (6). However, we can also apply the Fourier transform in the spatial domain. For instance, if a signal g is dependent on spatial coordinates of x, y, and z, i.e., $g = g(x, y, z)$, we can take its Fourier transforms with respect to the spatial coordinates, for example, x. We have

$$G(k_x, y, z) = \int_{-\infty}^{+\infty} g(x)e^{-jk_x x}dx \tag{11}$$

where k_x is the angular *spatial* frequency along the x-direction (similar to ω in the frequency domain). $f_x = k_x/2\pi$ is the spatial frequency in the x-direction (similar to f but measuring the number of spatial periods per unit length in the x-direction). If we take the Fourier transform simultaneously with respect to x, y, and z, we have

$$G(k_x, k_y, k_z) = \int_{-\infty}^{+\infty} g(x, y, z)e^{-j(k_x x+k_y y+k_z z)}dxdydz \tag{12}$$

where k_x, k_y, and k_z are the angular *spatial* frequencies along the x-, y-, and z-directions, respectively. They are also referred to as wave numbers or propagation constants in the literature. Again, the properties of Fourier transform operations, such as (8) and (9), apply.

Equations (11) and (12) are often called the signals or electromagnetic fields in the spectral domain. We can then

transform Helmholtz's equations (10) into the spectral domain by taking the Fourier transform with respect to the spatial coordinates x and y. This results in the following equation:

$$\begin{cases} \dfrac{d^2\tilde{\boldsymbol{E}}}{dz^2} + \left[\left(\dfrac{\omega}{c}\right)^2 - k_x^2 - k_y^2\right]\tilde{\boldsymbol{E}} = \dfrac{\nabla\tilde{\rho}}{\varepsilon} + j\omega\mu\tilde{\boldsymbol{J}} \\ \dfrac{d^2\tilde{\boldsymbol{H}}}{dz^2} + \left[\left(\dfrac{\omega}{c}\right)^2 - k_x^2 - k_y^2\right]\tilde{\boldsymbol{H}} = -\mu\nabla\times\tilde{\boldsymbol{J}} \end{cases} \tag{13}$$

where $\tilde{\boldsymbol{E}}, \tilde{\boldsymbol{H}}, \tilde{\rho}$, and $\tilde{\boldsymbol{J}}$ are the respective Fourier transforms of $\boldsymbol{E}, \boldsymbol{H}, \rho$, and $\boldsymbol{J}$. The advantage of (13) is that having the original three partial derivatives in the equations is now reduced to having one derivative, and (10) becomes an ordinary differential equation (ODE). The disadvantage is that to recover the solutions in the physical spatial domain of (x, y, z), (13) needs to be solved over the entire domain of $k_x \in [-\infty, +\infty]$ and $k_y \in [-\infty, +\infty]$ so that the inverse Fourier transform can be carried out.

III. Approximation in Inner Product Space and the MWR

We mentioned in the introduction that numerical methods do not, in general, yield mathematically exact solutions to Maxwell's equations due to their discretized nature. Instead, they *approximate* the exact solutions as closely as possible by following a procedure known as *the method of weighted residuals* (*MWR*), which has been developed for solving linear and nonlinear differential equations [16]. It involves two consecutive steps. The first consists of expressing the unknown solution as a sum of known (pre-selected) basis or expansion functions with unknown expansion coefficients. The second step determines these coefficients such that the approximation is as close as possible to the accurate solution [11], [17], [18].

The expression of the unknown solution as a sum of weighted basis functions is analogous to expressing a vector as a sum of components obtained by its orthogonal projection onto the coordinate axes of a Euclidian vector space, which involves forming the inner products of the vector with the unit basis vectors. The vector space and, by analogous extension to a function space, is thus referred to as an *inner product space* [12], which is usually a Hilbert space in electromagnetics.

In the following, we consider the properties of the inner product space and the MWR for finding the coefficients that yield approximations using the numerical methods used in electromagnetics.

A. Inner Product Space

Consider a function space $\boldsymbol{F}$ whose elements are a set of functions $\{f_i \,|\, i = 1, 2, \ldots\}$. An inner product space requires that the inner product operation, denoted as $\langle\cdot,\cdot\rangle$, on any functions f_1, f_2, and f_3 in $\boldsymbol{F}$ has the following four properties.

1) $\langle f_1, f_2\rangle = \overline{\langle f_2, f_1\rangle}$.
2) $\langle f_1 + f_2, f_3\rangle = \langle f_1, f_3\rangle + \langle f_2, f_3\rangle$ and $\langle f_1, f_2 + f_3\rangle = \langle f_1, f_2\rangle + \langle f_1, f_3\rangle$.
3) $\langle f_1, \alpha f_2\rangle = \bar{\alpha}\langle f_1, f_2\rangle$ and $\langle \alpha f_1, f_2\rangle = \alpha\langle f_1, f_2\rangle$.
4) $\langle f_1, f_1\rangle$ is a non-negative number and $\langle f_1, f_1\rangle = 0$ if and only if $f_1 = 0$.

Here, the bar over the symbols is the conjugate operator. If the function space is real, the bar sign can be removed since the conjugate of a real function is the function itself.

Property 1) is the conjugate symmetry, property 2) is the additivity, property 3) is the conjugate bilinearity, and property 4) is the positive definite property.

The inner product is most often defined as an integration over a problem domain, although other forms of the inner products may be used. The integration of two functions, or their inner product, $\langle f_1, f_2\rangle = \int_\Omega f_1 \bar{f}_2 d\Omega$, may also be interpreted as the similarity between two functions, or a measure of how much of f_1 is contained in f_2, or vice versa. Note that the inner product should be in vector form (e.g., integration of the dot product of two vectors) if two functions are vectors, such as vector basis and weighting functions.

B. Method of Weighted Residuals

Given the above properties of the inner product, the MWR can be used to generate a wide range of numerical methods [19], [20]. In the following paragraphs, we will discuss the MWR procedure, consisting of function expansion and determination of the unknown coefficients through the minimization of the so-called residuals (with another function expansion). A simple example will demonstrate the effectiveness of the method.

Maxwell's equations and their derivations such as (1), (2), (10), or (13) can be generalized as follows:

$$Lu(\mathbf{r}, t) - g(\mathbf{r}, t) = 0, \quad \mathbf{r} \in \Omega \tag{14}$$

where L is either a differential or integral operator, $u(\mathbf{r}, t)$ is an unknown signal or field function to be determined, $g(\mathbf{r}, t)$ is a known source or excitation function, $\mathbf{r}$ is the radial vector specifying the position, t is the time variable, and Ω is the solution domain which can be a boundary contour, a surface, or a 3-D volume. Note that for frequency domain solutions, t is replaced with the angular frequency ω.

The first step in the MWR procedure is to approximate the unknown solution $u(\mathbf{r}, t)$ with a trial function $\tilde{u}(\mathbf{r}, t)$ that can be represented as the expansion of a pre-selected set of basis functions $\{\varphi_n(\mathbf{r}, t), n = 1, 2, 3, \ldots\}$, as mentioned above. Mathematically

$$u(\mathbf{r}, t) \approx \tilde{u}(\mathbf{r}, t) = \sum_{n=1}^{N} a_n \varphi_n(\mathbf{r}, t) \tag{15}$$

with a_n being the expansion coefficients, and provided that $L\varphi_n(\mathbf{r}, t)$ forms a complete set in the range of L [21]– [23]. Equation (15) approximates the solution in a function space spanned by the basis functions $\{\varphi_n(\mathbf{r}, t), n = 1, 2, 3, \ldots\}$, reducing the task of finding the unknown solution to determining the expansion coefficients.

We now define the residual error $R(\mathbf{r}, t)$ in (16); it is caused by substituting the approximate solution or trial function $\tilde{u}(\mathbf{r}, t)$ into the original operator equation (14)

$$L\tilde{u}(\mathbf{r}, t) - g(\mathbf{r}, t) = R(\mathbf{r}, t), \quad \mathbf{r} \in \Omega. \tag{16}$$

The second step of the MWR procedure is to choose a set of weighting (or testing) functions $\{\omega_m(\mathbf{r}, t), m = 1, 2, 3, \ldots\}$

to expand the residual function $R(\mathbf{r}, t)$ and then make the resulting residual expansion coefficients equal to zero. That is,

$$\langle R(\mathbf{r}, t), w_m(\mathbf{r}, t)\rangle = 0. \tag{17}$$

The weighting functions $\{w_m(\mathbf{r}, t), m = 1, 2, 3, \ldots\}$ must be in the range of L and must span the function space of the source function $g(\mathbf{r}, t)$ as dictated by (16) [21]–[23]. If the weighting functions are chosen the same as the basis functions, the method is called a Bubnov–Galerkin procedure. If the basis and testing functions are different, it is called a Petrov–Galerkin procedure.

Substitution of the approximating trial function (15) into (17) and application of the properties of the inner product yield

$$\sum_{n=1}^{N} a_n \langle L\varphi_n, w_m\rangle = \langle g, w_m\rangle \tag{18}$$

which is a linear system of equations for the expansion coefficients a_n. Once the a_n are found, the approximate solution is obtained by (15) since both the expansion functions and their coefficients are now known.

Further issues such as solution convergence, errors, and computational expenditures will be discussed in Sections III-C and III-D.

C. Convergence

As the approximate solution (15) is given in terms of the basis functions, we must examine its convergence as the number of expansion terms N tends toward infinity

$$\tilde{u}(\mathbf{r}, t)|_{N\to\infty} = \lim_{N\to\infty} \sum_{n=1}^{N} a_n \varphi_n(\mathbf{r}, t) = f(\mathbf{r}, t) \tag{19}$$

where the converged function $f(\mathbf{r}, t)$ may or may not be the exact field solution $u(\mathbf{r}, t)$.

However, it is very challenging to develop necessary and sufficient convergence conditions for (19) that are applicable to all cases. Instead, we may be able to find specific conditions that are useful for checking convergence.

One of the necessary conditions is that the expansion coefficients a_n must be bounded

$$|a_n| < \infty \text{ for all } n, \text{ in particular, when } n \to \infty. \tag{20}$$

Since (18) yields the expansion coefficients a_n, the so-called "stability condition" can be derived from it. A specific mathematical form of the condition can only be derived on a case-by-case basis, as shown below.

D. Errors and Numerical Dispersion

The solution error function defined as the difference between the exact and the approximate solutions is

$$e(\mathbf{r}, t) = \tilde{u}(\mathbf{r}, t) - u(\mathbf{r}, t) = \sum_{n=1}^{N} a_n \varphi_n(\mathbf{r}, t) - u(\mathbf{r}, t). \tag{21}$$

Furthermore

$$\begin{aligned} L[e(\mathbf{r}, t)] &= L[\tilde{u}(\mathbf{r}, t) - u(\mathbf{r}, t)] \\ &= L[\tilde{u}(\mathbf{r}, t)] - L[u(\mathbf{r}, t)] \\ &= g(\mathbf{r}, t) + R(\mathbf{r}, t) - g(\mathbf{r}, t) = R(\mathbf{r}, t). \end{aligned} \tag{22}$$

Application of (17) yields

$$\langle L[e(\mathbf{r}, t)], w_m(\mathbf{r}, t)\rangle = 0. \tag{23}$$

Suppose that L^* is the adjoint of L. We then have

$$\langle e(\mathbf{r}, t), L^* w_m(\mathbf{r}, t)\rangle = 0. \tag{24}$$

Although (23) or (24) presents the equation for finding the error function $e(\mathbf{r}, t)$, solving it is very challenging in practice. Therefore, in most instances, numerical computations are compared directly with analytical solutions (if available), measurement results, or results obtained with other methods, whichever is available.

Alternatively, a frequently used approach is to consider the situation of source-free ($\mathbf{J} = 0$ and $\rho = 0$), homogeneous, free space. We then compare the propagation properties of the analytical field solutions with the approximate solutions obtained with the MWR in the frequency and spectral domains, as described below.

1) Spectral Properties of the Analytical Solutions in Free Space: In the source-free empty space, electromagnetic waves obey the wave equation (2), with the right-hand side being zero. We now apply the Fourier transform to (2) to time t and spatial coordinates x, y, z, respectively (note the Cartesian coordinates are taken for simplicity). We have

$$\begin{cases} \left(k_x^2 + k_y^2 + k_z^2 - k^2\right)\tilde{\boldsymbol{E}} = 0 \\ \left(k_x^2 + k_y^2 + k_z^2 - k^2\right)\tilde{\boldsymbol{H}} = 0 \end{cases} \tag{25}$$

where $k = \omega/c = \omega(\mu\varepsilon)^{1/2}$ is the wavenumber and $c = 1/(\mu\varepsilon)^{1/2}$ is the constant speed of light. $\tilde{\boldsymbol{E}}$ and $\tilde{\boldsymbol{H}}$ are the respective Fourier transforms of $\boldsymbol{E}$ and $\boldsymbol{H}$. Solutions of these equations for non-trivial $\tilde{\boldsymbol{E}}$ and $\tilde{\boldsymbol{H}}$ values must satisfy

$$k_x^2 + k_y^2 + k_z^2 - k^2 = 0 \Rightarrow k_x^2 + k_y^2 + k_z^2 = k^2. \tag{26}$$

The above equation is a sphere with the radius k in the k-space spanned by k_x, k_y and k_z. In spherical coordinates, we have

$$\begin{cases} k_x = k\cos\phi\sin\theta \\ k_y = k\sin\phi\sin\theta \\ k_z = k\cos\theta. \end{cases} \tag{27}$$

Here, ϕ and θ are the propagation angles if the electromagnetic wave is a plane wave.

Equation (26) represents the relationship between the spatial frequencies k_x, k_y, k_z and k for a constant propagation speed c of the exact solution $u(\mathbf{r}, t)$. It is often called the *analytical* dispersion relation.

For the approximate solutions obtained with the MWR method, the dispersion relation is, in general, not a perfect sphere of (26). It can be found by following this procedure.

Apply the Fourier transform to the approximate solution given by (15)

$$\begin{aligned}\tilde{U}\left(k_x, k_y, k_z, \omega\right) &= \mathcal{F}\left[\sum_{n=1}^{N} a_n \varphi_n(\mathbf{r}, t)\right] \\ &= \sum_{n=1}^{N} a_n \mathcal{F}[\varphi_n(\mathbf{r}, t)] \\ &= \sum_{n=1}^{N} a_n \Phi_n\left(k_x, k_y, k_z, \omega\right) \end{aligned} \tag{28}$$

where $\Phi_n(k_x, k_y, k_z, \omega) = \mathcal{F}[\varphi_n(\mathbf{r}, t)]$ is the temporal and spectral Fourier transform of the basis function $\varphi_n(\mathbf{r}, t)$.

Express the expansion coefficients a_n in terms of $\tilde{U}(k_x, k_y, k_z, \omega)$ and $\Phi_n(k_x, k_y, k_z, \omega)$ based on (28) and substitute the resulting expression into (23). The condition that leads to a non-trivial solution of $\tilde{U}(k_x, k_y, k_z, \omega)$ is then the dispersion of the MWR solution. We denote the condition henceforth as

$$f_d\left(k_x, k_y, k_z, \omega\right) = 0. \tag{29}$$

It depends on the expansion basis functions and weighting functions chosen.

If we consider a plane wave, (27) is substituted into the dispersion relation (29). We obtain

$$f_d(k\cos\phi\sin\theta, k\cos\phi\sin\theta, k\cos\theta, \omega) = 0. \tag{30}$$

The above equation allows us to solve for k and the wave speed $v = \omega/k$ for the approximate solution (15). v is usually a function of the propagation angles (ϕ, θ) and the frequency f, rather than the constant speed c of the analytical solution.

As mentioned before, the dispersion relation (30) of an MWR solution is usually not a sphere, which implies that the MWR solution is approximate. However, when the number of the expansion terms $N \to +\infty$, (30) should approach to being a sphere. If not, the approximate solution may not converge to a physical electromagnetic field solution but to some non-electromagnetic solutions, which are often called spurious solutions or -modes [24], [25].

For example, the well-known finite-difference time-domain (FDTD) method has the following numerical dispersion [26]:

$$\left[\frac{\sin\left(\frac{k_x \Delta x}{2}\right)}{\Delta x}\right]^2 + \left[\frac{\sin\left(\frac{k_y \Delta y}{2}\right)}{\Delta y}\right]^2 + \left[\frac{\sin\left(\frac{k_z \Delta z}{2}\right)}{\Delta z}\right]^2 = \left[\frac{\sin\left(\frac{\omega \Delta t}{2}\right)}{c\Delta t}\right]^2 \tag{31}$$

where Δx, Δy, Δz and Δt are the discretization steps in the x-, y-, z-, and t-direction, respectively. They are inversely proportional to the number of the expansion terms N of (15). When $N \to +\infty$, $\Delta x \to 0, \Delta y \to 0, \Delta z \to 0$, and $\Delta t \to 0$, the above dispersion relation approaches the sphere of the analytical solution (31). We can then say that the FDTD equations represent approximate solutions of Maxwell's equations.

In short, the analytical estimation of the errors of MWR solutions is quite challenging. In practice, the errors are evaluated on a case-by-case basis. Alternatively, spectral analysis in the frequency domain can be employed. The dispersion relationship between spatial frequencies, k_x, k_y, k_z, and ω, is first determined for the MWR solution, and the wave speed v is found from (30) and compared with the analytical speed, which is the constant speed of light c.

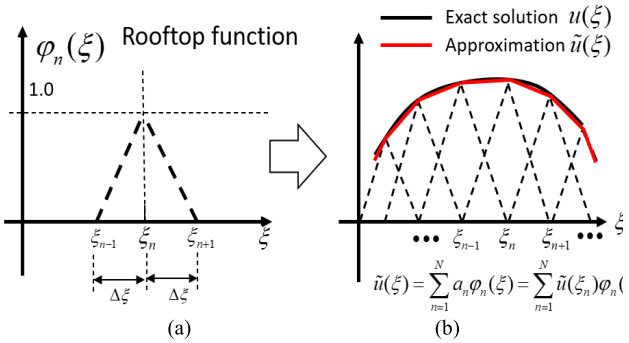

Fig. 2. (a) Typical rooftop function. (b) Trial function or approximate solution that is the sum of the rooftop functions.

IV. Unified View of Numerical Methods

With the above understanding and knowledge of the MWR, we now present the unified view of the most commonly used numerical methods in the following paragraphs. We divide the methods into two main categories: the frequency domain methods and the time-domain methods. Under each category, we apply the MWR to formulate their equations.

A. Frequency Domain Methods

As mentioned before, frequency-domain methods solve the Fourier-transformed time-domain electromagnetic field equations. In this article, we will focus on some of the best-known frequency-domain methods, namely, the finite difference method, the finite element method (FEM), the method of moments (MoM), the IE method, and the meshless method.

1) Finite Difference Method: Consider a function $u = u(\xi)$ where ξ is a spatial coordinate (e.g., x). We need to find its derivative $du/d\xi$.

We employ the rooftop function $\varphi_n(\xi)$, shown in Fig. 2(a), as the expansion or basis function. The rooftop function has the value of unity at its center point ξ_n and zero at its two edge nodes. The trial function or approximate solution, as illustrated in Fig. 2(b), can then be written as

$$u(\xi) \approx \tilde{u}(\xi) = \sum_{n=1}^{N} a_n \varphi_n(\xi) = \sum_{n=1}^{N} \tilde{u}(\xi_n)\varphi_n(\xi). \tag{32}$$

Because the rooftop function has the value unity at its center and zero at its edges, the associated expansion coefficient is equal to the approximate solution at the point ξ_n: $a_n = u_n(\xi_n)$.

Its derivative is then

$$\frac{du(\xi)}{d\xi} \approx \frac{d\tilde{u}(\xi)}{d\xi} = \sum_{n=1}^{N} a_n \frac{d\varphi_n(\xi)}{d\xi} = \sum_{n=1}^{N} \tilde{u}(\xi_n)\frac{d\varphi_n(\xi)}{d\xi} \tag{33}$$

which is the two-step pulse function depicted in Fig. 3.

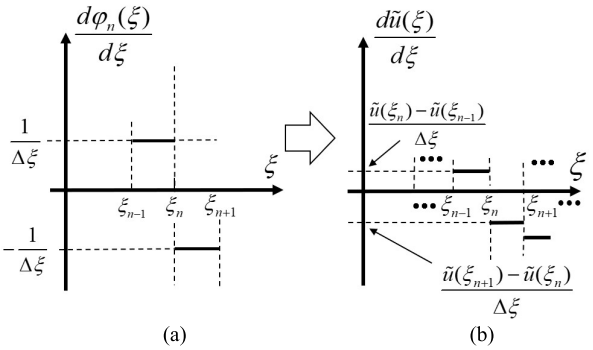

Fig. 3. (a) Derivative of the rooftop basis function. (b) Derivative of the the trial function.

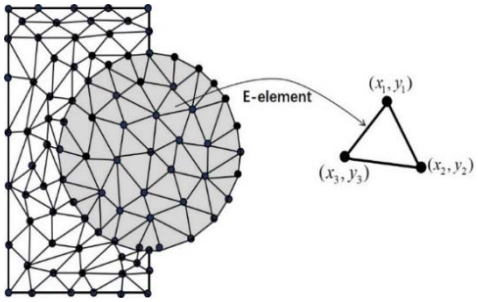

Fig. 4. Discretization in the FEM.

If we now choose the weighting function to be the Dirac impulse function $w_m = \delta(\xi - \xi_{m+1/2})$ and evaluate its inner product with (32), we get the approximate derivative

$$\begin{aligned}\frac{du(\xi)}{d\xi}\Big|_{\xi=\xi_{n+1/2}} &\approx \frac{d\tilde{u}(\xi)}{d\xi}\Big|_{\xi=\xi_{n+1/2}} \\ &= \left[u(\xi_n)\frac{d\varphi_n(\xi)}{d\xi} + u(\xi_{n+1})\frac{d\varphi_{n+1}(\xi)}{d\xi}\right]\Big|_{\xi=\xi_{n+\frac{1}{2}}} \\ &= \frac{u(\xi_{n+1}) - u(\xi_n)}{\Delta\xi}. \end{aligned} \tag{34}$$

The above equation is precisely the same as the conventional central finite-difference formulation [27].

2) Finite Element Method: The FEM can also be formulated in terms of the MWR method. For convenience, let us consider a 2-D case.

First, we divide the 2-D problem domain into triangular patches called elements, as shown in Fig. 4.

Consider a typical eth element. It has three vertices with coordinates $(x_i,\ y_i)$ where $i = 1, 2, 3$. In the FEM, three shape functions $s_{ei}(x, y)$ are used to expand the fields

$$\begin{cases} s_{e1}(x, y) = \dfrac{(x_2y_3 - x_3y_2) + (y_2 - y_3)x + (x_3 - x_2)y}{2A} \\ s_{e2}(x, y) = \dfrac{(x_3y_1 - x_1y_3) + (y_3 - y_1)x + (x_1 - x_3)y}{2A} \\ s_{e3}(x, y) = \dfrac{(x_1y_2 - x_2y_1) + (y_1 - y_2)x + (x_2 - x_1)y}{2A} \end{cases} \tag{35}$$

where A is the area of the element (triangular patch)

$$A = \frac{1}{2}\begin{vmatrix} 1 & x_1 & y_1 \\ 1 & x_2 & y_2 \\ 1 & x_3 & y_3 \end{vmatrix} \tag{36}$$

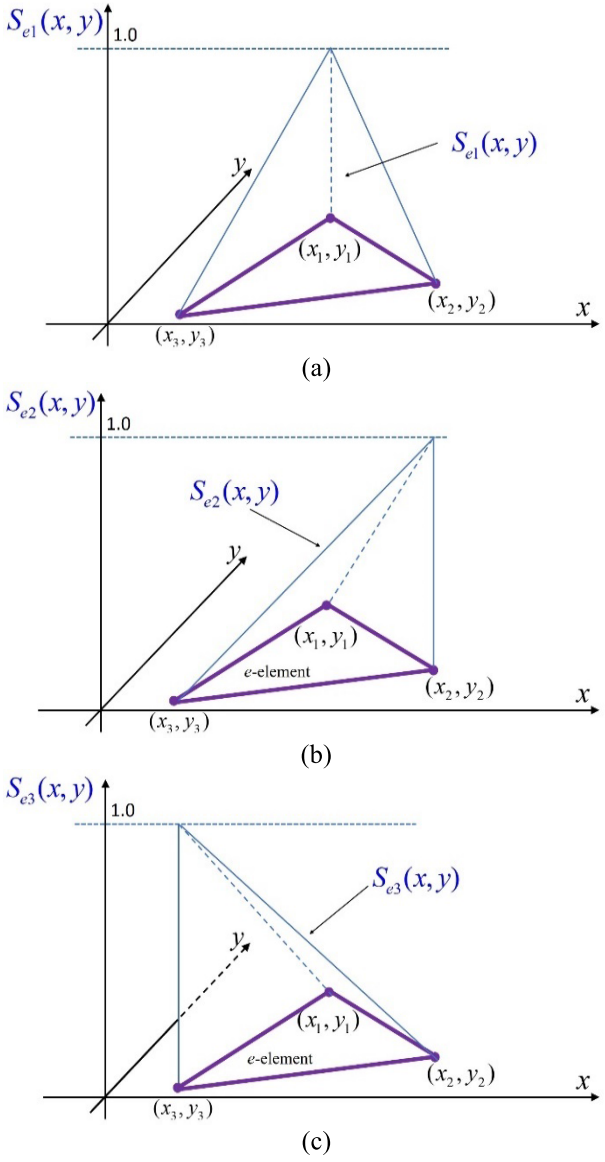

Fig. 5. Shape functions of a triangular element. (a) Shape function $S_{e1}(x, y)$. (b) Shape function $S_{e2}(x, y)$. (c) Shape function $S_{e3}(x, y)$.

$s_{ei}(x, y, z)$ pertains to the ith vertex of the element which is pictured in Fig. 5. It has Kronecker properties

$$s_{ei}(x_l, y_l) = \begin{cases} 1, & \text{when } l = i \\ 0, & \text{when } l \neq i. \end{cases} \tag{37}$$

It states that the shape function has the values of unity at one vertex and zero at any other two vertices, as shown in Fig. 5.

In the FEM, we use the shape functions as the basis functions in each element. The approximate solution (15) becomes

$$u(\mathbf{r}, t) \approx \tilde{u}(\mathbf{r}, t) = \sum_{n=1}^{N} a_n\varphi_n(\mathbf{r}, t) = \sum_{e=1}^{N_e}\sum_{i=1}^{3} a_{ei}s_{ei}(x, y) \tag{38}$$

where $\varphi_n(\mathbf{r}, t) = s_{ei}(x, y), n = 3(e - 1) + i$. e refers to the element and i to the vertex. The projective approximation (38) then becomes the sum of the shape functions of all the elements. By virtue of the Kronecker properties (39) of the shape function, the expansion coefficients a_{ei} become

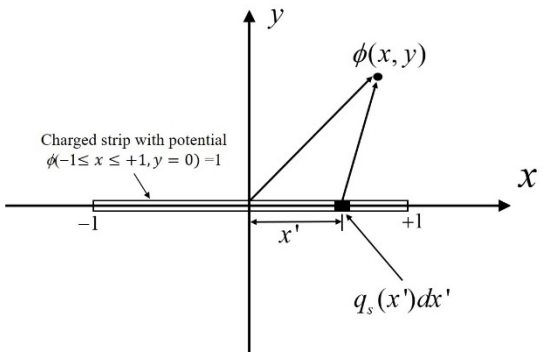

Fig. 6. Charged strip with a unity potential.

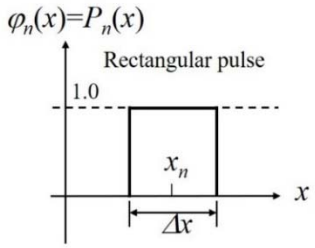

Fig. 7. Rectangular pulse functions are selected as basis functions.

$a_{ei} = \tilde{u}(\mathbf{r}_i, \omega) = \tilde{u}(x_i, y_i, \omega)$, which are the approximate field values at the element vertices.

We now substitute (38) into the operator equation and obtain the residual. We then select suitable weighting functions $\{w_m(\mathbf{r}, t), m = 1, 2, 3, \ldots\}$ to expand the residual function and minimize the residual by forcing the residual expansion coefficient to become zero. A frequent choice of the weighting functions is Dirac impulse functions centered at the element vertices

$$\delta(x_i, y_i) = \delta(x - x_i)\delta(y - y_i) = \begin{cases} \infty, & \text{when } x = x_i \text{ and } y = y_i \\ 0, & \text{when } x \neq x_i \text{ or } y \neq y_i \end{cases} \quad (39)$$

with the property of

$$\int_{x_i^-}^{x_i^+}\int_{y_i^-}^{y_i^+} \delta(x, y)dxdy = \int_{x_i^-}^{x_i^+}\int_{y_i^-}^{y_i^+} \delta(x - x_i)\delta(y - y_i)dxdy = 1.$$

Another common choice of weighting function is the shape function $s_{ei}(x, y, z)$, resulting in Bubnov Galerkin's method.

The reader can find more information about the FEM for electromagnetic modeling in the existing large body of literature, including [28]. Note that different notations are used for the basis functions or shape functions in different reports.

3) Method of Moments: Harrington [29] wrote an excellent book, *Field Computation by Moment Methods*, the classical text still being used today. The MoM is traditionally applied to the IEs that are derived from Maxwell's equation. The solution follows the two-step process of the MWR, as described in Section II. Therefore, the MoM is a form of the MWR. Readers are referred to published literature on the subject such as [30].

4) Integral Equation Methods: The IE methods are popular for solving open electromagnetic problems [31]. We can derive many forms of the IEs from Maxwell's equations, resulting in many IE approaches. Some solve for the field quantities, while others solve for the currents or charges [32]. As a result, different IE methods may be best suited for different structures, depending on the quantities to be solved.

For illustration purposes, consider a charged strip in the static case ($\omega = 0$), as shown in Fig. 6.

The following expression for the potential can be derived from Maxwell's equations:

$$\phi(x, y) = \frac{1}{2\pi\varepsilon}\int_{-1}^{+1} q_s(x') \ln \frac{1}{\sqrt{(x - x')^2 + y^2}} dx' \quad (40)$$

where $q_s(x')$ is the unknown linear surface charge density of the strip. $\phi(x, y)$ is the potential generated by the charged strip.

Suppose the potential on the strip is 1 V. The boundary condition for the potential function (40) is thus

$$\phi(-1 \le x \le +1, y = 0) = 1.0. \quad (41)$$

The operator equation (14) for the linear surface charge density $q_s(x')$ then becomes

$$\frac{1}{2\pi\varepsilon}\int_{-1}^{+1} q_s(x') \ln \frac{1}{|x - x'|} dx' - 1 = 0. \quad (42)$$

Following the MWR procedure, we can find an approximate solution for $q_s(x')$. Once $q_s(x')$ is obtained, we can find the potential at any location (x, y) with (40). The electric field $\mathbf{E}$ is then $\mathbf{E} = -\nabla\phi(x, y)$.

Now let us define uniformly sampling points on the strip, $\{x_1, x_2, \ldots, x_n, \ldots, x_N\}$, $x_n = -1 + \Delta x/2 + (n-1)\Delta x$, $\Delta x = 2/N$. N is the number of discrete sampling points. We then choose rectangular pulse functions, $\varphi_n(x) = P_n(x)$, centered at the sampling points x_n with the pulse width of $\Delta x = 2/N$, as the basis functions (shown in Fig. 7).

Furthermore, we select the Dirac delta impulse function, also centered at the sampling point x_m, as the weighting function, $w_m(x) = \delta(x - x_m)$, $m = 1, 2, 3, \ldots, N$. After some mathematical manipulations, we obtain the following system of linear equations for the expansion coefficients a_n:

$$\sum_{n=1}^{N} c_{mn} a_n = 2\pi\varepsilon, \quad m = 1, 2, 3, \ldots, N \quad (43)$$

where

$$c_{mn} = (x_m - x_n)\ln\left(|x_m - x_n - \frac{\Delta x}{2}|/|x_m - x_n + \frac{\Delta x}{2}|\right) + \frac{\Delta x}{2}\ln\left(1/|(x_m - x_n)^2 - \left(\frac{\Delta x}{2}\right)^2|\right) + \Delta x. \quad (44)$$

With the solution of (43) for the expansion coefficients a_n, we plot the approximate solutions for an increasing number of sampling points N in Fig. 8.

The above example is a simple 1-D case. In a more general case, an electric field IE (EFIE) [33] (or a magnetic field IE MFIE [34]) in vector form is developed first from Maxwell's equations

$$L[\mathbf{E}(\mathbf{r})] - \mathbf{g}(\mathbf{r}) = 0 \quad (45)$$

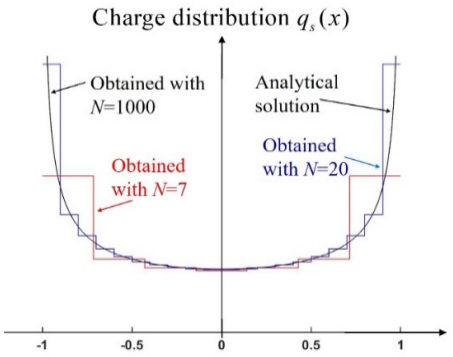

Fig. 8. Computed charge distribution for different numbers of expansion terms.

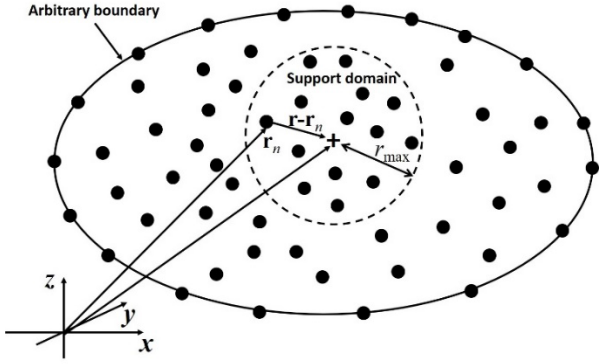

Fig. 9. Support domain of a point of interest and its surrounding nodes.

where L is likely an integration operator similar to (42) but in vector form. $\mathbf{g}$ is also a vector function.

We then follow the MWR process with the note that the projection and expansion of (15) are now in vector form: the basis and weighting functions and the inner product are all vectors

$$\mathbf{u}(\mathbf{r},\omega)=\mathbf{E}(\mathbf{r},\omega)\approx\tilde{\boldsymbol{E}}(\mathbf{r},\omega)=\sum_{n=1}^{N}a_n\boldsymbol{\varphi}_n(\mathbf{r},\omega). \tag{46}$$

For more details and more complex problems, readers are referred to [31] and [35]–[37].

5) Spectral Domain Method: The spectral domain method is a specialized numerical method that solves electromagnetic problems in the spectral domain (as described in Sections II-C and III-D). It can be efficiently applied to planar structures, such as microstrip lines [38]. Starting with Helmholtz's equation (10) in the frequency domain, an IE is derived with current densities or charges being the unknown quantities to be solved for. The current or charge densities are then expanded in terms of the pre-selected basis functions with unknown expansion coefficients. The MWR process is applied, and a system of linear equations is obtained for the expansion coefficients. The core of the spectral-domain method is that the expansion coefficients are efficiently found through the use of Green's functions in the spectral (or spatial frequency) domain rather than directly in the spatial domain. Chen and Ney [19] present a good description of the spectral domain method with the MWR (or MoM). Therefore, the spectral domain method lies within the framework of the MWR. Note that in formulating the expansion and computing the expansion coefficients in the spectral domain, Parseval's theorem is applied to show the orthogonality of the basis function, convergence, and integration limits. The details can be found in [10] and [38].

6) Meshless Methods: Conventionally, numerical methods are developed by discretizing a continuous solution domain into small cells or geometrical shapes, often called mesh or grid. For example, in a 2-D FEM, triangular meshes are used, as discussed before. In a 3-D FEM, we use tetrahedral meshes. In a 2-D finite difference method, we use a rectangular mesh, and in a 3-D finite difference method, we use cuboid meshes. Vertices of these meshes or grids must follow certain rules or relationships to enable the discretization with numerical cells.

In contrast, meshless methods do not employ structured meshes, as their name suggests [39], [40]. Instead, we first choose spatial nodes located throughout a solution domain, and then we select the basis functions that are centered at or associated with these nodes. We now follow the MWR process to obtain the meshless formulation. Fig. 9 shows an example.

In Fig. 9, we choose the spatial nodes, marked with +, in the domain. We define a support domain of radius $r_{\max}$ centered at a point of interest within which we project the solution in terms of the radial and monomial basis functions as follows:

$$u\approx\tilde{u}(\mathbf{r})=\sum_{n=1}^{N_1}R_n(\mathbf{r})a_n+\sum_{n=N_1+1}^{N}P_n(\mathbf{r})a_n \tag{47}$$

where $\mathbf{r}=(x,y,z)$ are the coordinates of the point of interest at which the field value u is to be approximated. $R_n(\mathbf{r})$ is a radial basis function, $P_n(\mathbf{r})$ is a monomial basis function, and a_n are the expansion coefficients. N_1 is the number of nodes in the support domain of $\mathbf{r}$ that determines the number of radial basis functions used to find $\tilde{u}(\mathbf{r})$. Very often, the Gaussian function is adopted for the radial basis [41]. It is an exponential function of distance with shape parameter α that controls the decay rate

$$R_n(\mathbf{r})=e^{-\alpha(|\mathbf{r}-\mathbf{r}_n|/r_{\max})^2} \tag{48}$$

where $|\mathbf{r}-\mathbf{r}_n|=((x-x_n)^2+(y-y_n)^2+(z-z_n)^2)^{1/2}$, $\mathbf{r}_n=(x_n,y_n,z_n)$ are the coordinates of the nth node within the support domain of the point of interest $\mathbf{r}$.

By forcing (47) to pass through every node in the support domain, we can obtain the approximate fields at the nodes within the support domain

$$u\approx\tilde{u}(\mathbf{r})=\sum_{n=1}^{N_1}R_n(\mathbf{r})a_n+\sum_{n=N_1+1}^{N}P_n(\mathbf{r})a_n=\sum_{n=1}^{N_1}\varphi_n(\mathbf{r})\tilde{u}_n \tag{49}$$

where $\tilde{u}_n=\tilde{u}(\mathbf{r}=\mathbf{r}_n)$ is the approximate field value at the node $\mathbf{r}_n$ within the support domain. $\varphi_n(\mathbf{r})$ is the shape function associated with $\mathbf{r}_n$, and it has the following Kronecker property:

$$\varphi_n(\mathbf{r})=\begin{cases}1, & \text{at node } \mathbf{r}_n \text{ (i.e., } \mathbf{r}=\mathbf{r}_n)\\ 0, & \text{at other nodes (i.e., } \mathbf{r}=\mathbf{r}_m \text{ and } m\neq n).\end{cases} \tag{50}$$

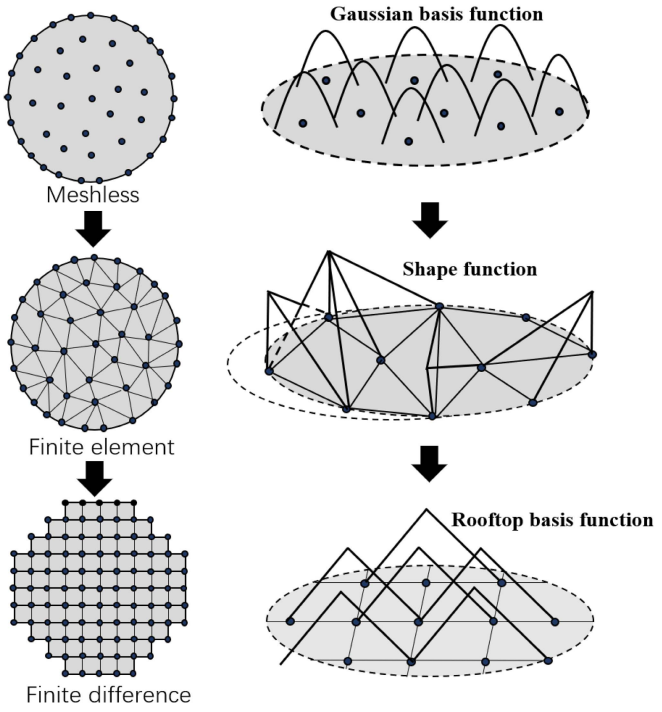

Fig. 10. Illustration of the node-based meshless method (top figure) and its evolution into the FEM (middle figure) and the finite difference method (bottom figure).

Once we establish the projective expansion of (49) and (50), we can proceed with the MWR process and obtain the node-based meshless method. A frequently used weighting function used is the Dirac delta impulse function that is centered at the nodes, respectively

$$w_m(\mathbf{r}) = \delta(\mathbf{r} - \mathbf{r}_m) = \begin{cases} \infty, & \text{when } \mathbf{r} = \mathbf{r}_m \\ 0, & \text{when } \mathbf{r} \neq \mathbf{r}_m. \end{cases} \tag{51}$$

More details about the meshless formulation can be found in [39], [40], [42], and [43].

The node-based meshless method allows great flexibility in the placement of the spatial nodes. As a result, arranging them in a specific pattern can lead to a particular method that we commonly know [44]. For instance, if we connect the nodes with straight lines in a 2-D case, we will discretize the solution domain into triangular patches. If we further employ shape functions within the patches as the basis functions, the meshless method becomes the FEM. If we arrange the nodes on a rectangular grid and employ rooftop functions as basis functions, we will obtain the finite-difference method. Fig. 10 shows the evolution of the meshless method into the FEM and the finite difference method. In other words, we can use the node-based meshless method to generalize different numerical methods and thus to serve as a unifying framework for the derivation and characterization of a group of numerical methods.

Note that in the above node-based meshless derivations, scalar basis functions are considered for illustration simplicity. In addition to the scalar functions, methods using vector basis functions have been developed, for instance, the popular edge FEM [28] (and references therein). Since these vector basis functions can be associated with spatial nodes or grid points directly or indirectly, the methods formulated with the vector basis functions can be found as special cases of the general node-based meshless method. In the case of the edge FEM, on the surface, the vector basis functions are only associated with the edges, but two ends of an edge are the nodes. Therefore, every vector basis function, in reality, is also associated with the nodes. If we consider the expansion at a node as the combinations of the vector basis functions of all the edges that are connected to the node, the edge FEM is then the special case of the node-based FEM in the vector form. In addition, the inner product is the dot product of two vector functions. The expansion coefficients of the vector basis functions are the unknown quantities to be found. In other words, the node-based meshless method can be used to develop the edge FEM with the special selection of the basis functions and inner product.

B. Time-Domain Methods

As their name indicates, time-domain methods essentially solve electromagnetic problems in the time domain. That is, they are used to find approximate solutions to time-dependent electromagnetic equations (16). Since frequency domain electromagnetic equations are the Fourier transform of the associated time-domain electromagnetic equations, there exists a corresponding frequency-domain method for every given time-domain method and vice versa. As we have discussed the finite-difference method, FEM, moment method, IE method, and the meshless method in the frequency domain in Section IV-A, we will discuss their time-domain counterparts in Section IV-B. The names of these methods are the same as those in Section IV-A but with the added "time-domain" attribute. Moreover, we will discuss another powerful method, the (time-domain) transmission-line-matrix (TLM) method, that was developed originally in the time domain. Naturally, there also exists a frequency-domain TLM method, which the reader may further explore in [45].

There are two approaches to finding time-domain solutions: one is to employ a frequency domain method, find the solution in the frequency domain, and perform the inverse Fourier transform to get the time-domain solution; the other is to formulate and solve electromagnetic problems directly in the time domain. The former is inefficient in general since the inverse Fourier transform requires many frequency-domain solutions over a vast frequency band. The latter is more efficient since it solves the approximate time-domain solution directly in a single computation run. We can then perform the Fourier transform of the time-domain solution and obtain the frequency-domain solution. In the following paragraphs, we discuss the latter approach.

1) Finite-Difference Time-Domain Method: The FDTD method is the counterpart of the finite difference method in the frequency domain. It is formulated by directly applying (34) to the time differential operator. More details of the derivation of the FDTD method can be found in [26] and [46].

Note that (34) is the same central finite-difference operator that we conventionally derive from Taylor's series [27].

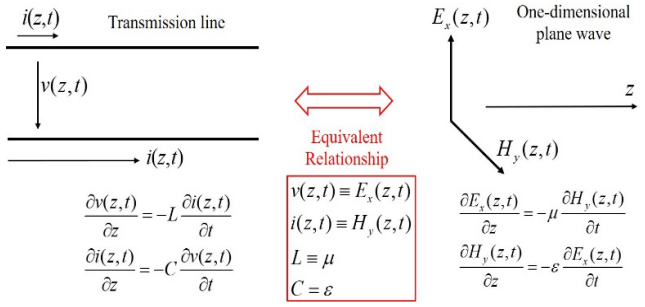

Fig. 11. Analogy between the transmission line and a plane way (or 1-D problem).

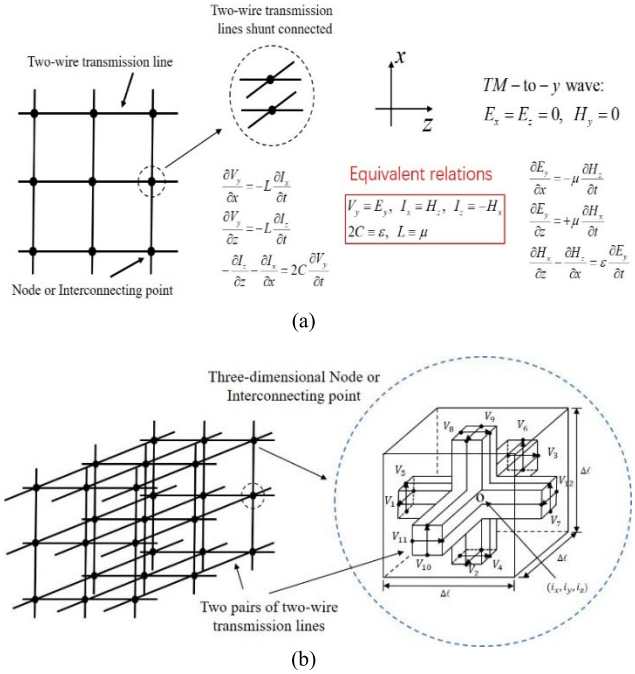

Fig. 12. Two- and three-dimensional TLM method. (a) Two-dimensional TLM and (b) three-dimensional TLM.

However, in the context of the MWR, the field expansion of (32) also presents the continuous field values at all spatial points in addition to those at the nodes (or grid points). The conventional finite-difference operator does not provide such information. That is an important advantage of the unifying MWR framework over the conventional approach.

2) Transmission Line Matrix Method: The TLM method originates from the analogy between voltages and currents in transmission lines and electric and magnetic fields in space [47], [48]. It is well known that these voltages and currents are governed by the telegrapher's equations which are of the same form as those describing electric and magnetic fields of a plane wave (typical for 1-D electromagnetic problems). Therefore, we can exploit the correspondence between transmission line parameters and the field quantities to find field solutions by solving the telegrapher's equation. Fig. 11 shows the analogy between transmission line and plane wave propagation. Using a transmission line model for solving 1-D electromagnetic field problems is advantageous because most readers are familiar with transmission line formalism and the equivalent circuit models commonly used to represent transmission line networks.

While the model of Fig. 11 is 1-D, we can extend the transmission line model to two and three spatial dimensions by interconnecting the transmission lines to form spatial networks, resulting in the so-called 2-D [see Fig. 12(a)] [49] and 3-D [see Fig. 12(b)] TLM models [50]. The interconnection points, called TLM nodes, are distributed over an entire solution domain.

The TLM methods use Dirac delta voltage impulses to sample the field quantities. A TLM simulation thus becomes a rather simple propagation process involving individual pulses traveling on the transmission lines linking two neighboring TLM nodes and being scattered at the TLM nodes. The electric and magnetic fields correspond directly to the impulse voltages and currents at the nodes and on the transmission link lines. Details of the TLM methods can be found in [48] and [51].

Although the TLM method was originally developed using transmission line concepts, it is equivalent to the FDTD method and can also be derived via the MWR [52], [53]. In other words, the unifying mathematical framework of the MWR approach includes the TLM method as well.

3) Time-Domain Finite-Element Method: The time-domain finite-element method (TD-FEM) is the FEM's counterpart in the frequency domain. It is formulated by directly applying (34) to the time differential operator in the formulations. Equation (34) is conventionally called the central finite-difference operator but has been derived with the MWR in this article. In the spatial domain, the TD-FEM conventionally applies the MWR process like in its frequency-domain counterpart. Therefore, the MWR is the unifying mathematical framework of the TD-FEM. More details of the derivation of the TD-FEM method can be found in [28] and [54].

The popular time-domain discontinuous Galerkin (DGTD) methods are a special case of the FEMs, in which the function space consists of piecewise continuous polynomials. These polynomials are allowed to be completely discontinuous across element interfaces. The DG methods can be regarded as the most extreme case of nonconforming FEMs, that is, a one-element one-domain scheme. DG was first proposed to solve the hyperbolic equation encountered in neutron transport [55] and was further developed by Cockburn and Shu [56]. Extensive applications of DG methods can be found in electromagnetics, fluid dynamics, elastic wave modeling, etc. The spirit of the DG method is to use the flux to relax the continuity condition between adjacent elements. It has been employed and applied in solving electromagnetic structure problems [57]. Its formulation follows the FEM and therefore falls into the framework of the MWR.

4) Time-Domain IE Methods: Time-domain integral equation (TDIE) methods can be considered as a specific application of the MoM procedure to TDIEs at each time step. Recognizing that the MoM is a significant element of the unified framework of computational electromagnetics, TDIEs belong to this framework as well. Bennett and Weeks [58] first proposed the TDIE method in 1968 in the form of a marching-

on-in-time (MOT) solution [59]. Using so-called Rao–Wilton–Glisson (RWG) basis functions as spatial and temporal basis functions facilitates the development of the MOT scheme [60]. The challenges are to overcome late-time instabilities and high computational costs. The incorporation of implicit schemes can remove the need to satisfy the Courant–Friedrichs–Lewy (CFL) stability condition and mitigate the late-time instability issue [61].

Let us consider the time-domain EFIE for the electromagnetic fields scattered by a perfectly electrically conducting (PEC) body with the enclosing surface S [62]

$$-\hat{n}(\mathbf{r}) \times \left[\hat{n}(\mathbf{r}) \times \partial_t \mathbf{E}^{\mathbf{inc}}(\mathbf{r}, t)\right] = -\hat{n}(\mathbf{r}) \times \left\{\hat{n}(\mathbf{r}) \times \left[\partial_t^2 \mathbf{A}(\mathbf{r}, t) + \nabla \partial_t \Phi(\mathbf{r}, t)\right]\right\} \quad (52)$$

where $\hat{n}(\mathbf{r})$ is an outward directed unit vector normal to S, ∂_t represents the time derivative, and $\mathbf{A}(\mathbf{r}, t)$ and $\Phi(\mathbf{r}, t)$ are the vector and scalar potentials

$$\{\mathbf{A}(\mathbf{r}, t), \Phi(\mathbf{r}, t)\} = \left\{ \iint_S \frac{\mu \mathbf{J}\left(\mathbf{r'}, t - \frac{R}{c}\right)}{4\pi R} ds', - \iint_S \int_0^{t - \frac{R}{c}} \frac{\nabla' \cdot \mathbf{J}(\mathbf{r'}, t')}{4\pi \varepsilon R} dt' ds' \right\}. \quad (53)$$

Here, $\mathbf{J}(\mathbf{r}, t)$ is the surface current density, $R = |\mathbf{r} - \mathbf{r'}|$ is the distance between the source point $\mathbf{r'}$ and observation point $\mathbf{r}$, and $c = 1/(\varepsilon \mu)^{1/2}$ is the speed of light.

To numerically solve the EFIE in the time domain, $\mathbf{J}(\mathbf{r}, t)$ is expanded with $N_s N_t$ space–time basis functions

$$\mathbf{J}(\mathbf{r}, t) \cong \sum_{k'=1}^{N_s} \sum_{l'}^{N_t} I_{k',l'} S_{k'}(\mathbf{r}) T\left(t - l' \Delta t\right) \quad (54)$$

where $I_{k',l'}$ are unknown expansion coefficients, and $\Delta t = \beta / f_{\max}$ is the time step with β being typically $0.02 \leq \beta \leq 0.1$ for a given maximum frequency $f_{\max}$. In general, the spatial and temporal basis functions $S_{k'}(\mathbf{r})$ and $T(t)$ are local; they have non-zero values only within a specific range.

Applying a spatial Galerkin procedure at $t = t_j = j \Delta t$, the following matrix equation is obtained:

$$\mathbf{Z}_0 \mathbf{I}_l = \mathbf{V}_l^{\text{inc}} - \sum_{l' = \max\left(1, l - N_g\right)}^{l-1} \mathbf{Z}_{l-l'} \mathbf{I}_{l'} = \mathbf{V}_l^{\text{inc}} - \mathbf{V}_l^{\text{scat}}, \quad l = 1, 2, \ldots, N_t. \quad (55)$$

The integer N_g is chosen in such a way that it approximates the longest possible transit time of the field produced by a temporal basis function across S. Detailed expressions of vectors and matrix elements can be found in [62] and [63].

The above solution process follows the two-step MWR procedure. Different approaches have been researched to improve the performance of the MOT scheme, including the following.

1) Improvement of temporal basis function $T(t)$ (e.g., [64]).
2) Improvement of spatial basis functions $S_{k'}(\mathbf{r})$ (e.g., [65]).
3) Adoption of extension to different IEs (e.g., [66], [67]).

It should be highlighted that the MOT scheme requires $O(N_t N_S^2)$ operations and $O(N_S^2)$ memory. Here, N_S and N_t are the number of spatial basis functions and the number of time steps, respectively. Such high computational complexity and memory requirements must be reduced for efficient simulation of electrically large and complex problems.

5) Time-Domain Meshless Method: The time-domain meshless method is the counterpart of the frequency-domain meshless method described in Section IV-A6 [39], [40], [43]. The only difference is that their finite-difference or numerical integration counterparts replace the standard time-differential or integral operators. Both operations can be viewed as the result of applying the MWR process. In other words, the time-domain meshless method can also be derived within the MWR framework.

V. Summary and Conclusion

In this article, we present a unified theoretical framework for numerical methods in electromagnetics. Each method approximates the unknown electromagnetic solution by a sum of weighted basis functions of a selected and method-specific function space. The unknown coefficients must be determined such that the difference (residual error) between the approximate and the exact solution is minimized. The residual error is minimized by expanding it in the function space formed by the weighting functions and making the expansion coefficients zero.

We discussed the most common numerical methods and described their derivation through the projection and residual minimization processes. We also demonstrated the relationships between frequency-domain and time-domain solutions, the physical meaning of solution convergence (or numerical stability), and error estimations. In particular, we demonstrated that in the case of free-space problems, the numerical dispersion errors result from approximation errors in the spectral domain.

To fully utilize a numerical method, one needs to know its pros and cons. A paper by Sankaran [68] presents quite well the advantages and disadvantages of various methods with an extensive discussion of flexibility, accuracy, and computational loads. To deal with computational expenses, many fast algorithms have been developed; they accelerate solution processes for modeling electrically large and complex problems [69]; they include multilevel fast multipole algorithm (MLFMA) [70]–[72], fast direct solution methods [73], [74], graphics processing unit (GPU) accelerated methods [75], [76], discontinuous Galerkin (DG) methods [57], [77], domain decomposition (DD) methods [78], and so on [79], [80]. Note that GPU acceleration is not exclusively a matter of technology but also requires a modification of the computational procedure and implementation scheme to run on specialized hardware.

Furthermore, the "second-level" projection techniques for reducing the dimensions of the solution spaces to achieve fast computations and small computational load have been developed, e.g., Krylov space [81]. Since this article focuses on the fundamental formulation with the MWR or the first-level projection, we do not elaborate on the details of the various acceleration methods, which would unduly increase the length of this article.

In summary, we have proposed a unified mathematical framework that is shared by all current numerical methods for solving Maxwell's equations. Each numerical method

developed so far employs its own specific set of basis functions to expand the unknown solutions of a problem and weighting or testing functions to project and then minimize the residual error with the MWR. This unified view facilitates the understanding of various numerical methods and the differences between them and provides a common and comprehensive methodology for presenting existing methods and for developing new numerical methods (including multiphysics modeling). Furthermore, we expect that the unified view will lead to the creation of a unifying computational platform for hybridizing all numerical methods.

This article is also intended to serve as a starting point for further research on the unification of the numerical methods with many questions that still need to be answered; for instance, what are the conditions on the function spaces for expanding the solutions and the residual functions? What are the criteria for the convergence of the projection approximation? What are the proper forms of the inner product for a specific electromagnetic problem? These questions are the subjects of further research and reports.

Further references on the theories and applications of finite-difference methods, meshless methods, projection methods, and their implementations are also listed in references for the benefit of readers who wish to research the subject of this article in greater detail [80]–[90].

REFERENCES

[1] J. C. Maxwell, *A Treatise on Electricity and Magnetism*. London, U.K.: Clarendon Press, 1873.

[2] O. Heaviside, *Electromagnetic Theory*. Providence, RI, USA: Amer. Math. Soc., 2003.

[3] H. Hertz, *Electric Waves: Being Researches on the Propagation of Electric Action With Finite Velocity Through Space*. New York, NY, USA: Dover, 1893.

[4] W. C. Chew, A. Y. Liu, C. Salazar-Lazaro, and W. E. I. Sha, "Quantum electromagnetics: A new look—Part I," *IEEE J. Multiscale Multiphys. Comput. Techn.*, vol. 1, pp. 73–84, 2016.

[5] W. C. Chew, A. Y. Liu, C. Salazar-Lazaro, and W. E. I. Sha, "Quantum electromagnetics: A new look—Part II," *IEEE J. Multiscale Multiphys. Comput. Techn.*, vol. 1, pp. 85–97, 2016.

[6] M. N. Sadiku, *Elements of Electromagnetics*. Oxford, U.K.: Oxford Univ. Press, 2014.

[7] D. Jackson, *The Theory of Approximation*. Providence, RI, USA: Amer. Math. Soc., 1930.

[8] H. N. Mhaskar and D. V. Pai, *Fundamentals of Approximation Theory*. Boca Raton, FL, USA: CRC Press, 2000.

[9] M. J. D. Powell, *Approximation Theory and Methods*. Cambridge, U.K.: Cambridge Univ. Press, 1981.

[10] T. Itoh, *Numerical Techniques for Microwave and Millimeter-wave Passive Structures*. New York, NY, USA: Wiley, 1989, p. 707.

[11] B. A. Finlayson, *The Method of Weighted Residuals and Variational Principles*. Philadelphia, PA, USA: SIAM, 2013.

[12] F. R. Deutsch, *Best Approximation in Inner Product Spaces*. New York, NY, USA: Springer, 2012.

[13] W. J. R. Hoefer, "Computational time reversal—A frontier in electromagnetic structure synthesis and design," *IEEE Trans. Microw. Theory Techn.*, vol. 63, no. 1, pp. 3–10, Jan. 2015.

[14] W. C. Chew, Y. Wang, G. Otto, D. Lesselier, and J.-C. Bolomey, "On the inverse source method of solving inverse scattering problems," *Inverse Problems*, vol. 10, no. 3, p. 547, 1994.

[15] A. D. Poularikas, *Transforms and Applications Handbook*. Boca Raton, FL, USA: CRC Press, 2018.

[16] S. Chakraverty, *Advanced Numerical and Semi Analytical Methods for Differential Equations*. Hoboken, NJ, USA: Wiley, 2019.

[17] M. H. Baluch, M. F. N. Mohsen, and A. I. Ali, "Method of weighted residuals as applied to nonlinear differential equations," *Appl. Math. Model.*, vol. 7, no. 5, pp. 362–365, Oct. 1983.

[18] B. Finlayson and L. Scriven, "The method of weighted residuals—A review," *Appl. Mech. Rev*, vol. 19, no. 9, pp. 735–748, 1966.

[19] Z. Z. Chen and M. M. Ney, "The method of weighted residuals: A general approach to deriving time- and frequency-domain numerical methods," *IEEE Antennas Propag. Mag.*, vol. 51, no. 1, pp. 51–70, Feb. 2009.

[20] Z. Chen, Y.-Q. Yu, and M. M. Ney, "The time-domain method of weighted residuals (MWR): Moving from grid-based methods to node-based meshless techniques," in *Proc. Int. Conf. Electromagn. Adv. Appl.*, Sep. 2009, pp. 200–203.

[21] A. Djordjevic and T. Sarkar, "A theorem on the moment methods," *IEEE Trans. Antennas Propag.*, vol. AP-35, no. 3, pp. 353–355, Mar. 1987.

[22] T. Sarkar, "A note on the choice weighting functions in the method of moments," *IEEE Trans. Antennas Propag.*, vol. AP-33, no. 4, pp. 436–441, Apr. 1985.

[23] T. Sarkar, A. Djordjevic, and E. Arvas, "On the choice of expansion and weighting functions in the numerical solution of operator equations," *IEEE Trans. Antennas Propag.*, vol. AP-33, no. 9, pp. 988–996, Sep. 1985.

[24] D. Sun, J. Manges, X. Yuan, and Z. Cendes, "Spurious modes in finite-element methods," *IEEE Antennas Propag. Mag.*, vol. 37, no. 5, pp. 12–24, Oct. 1995.

[25] J. S. NieLsen and W. Hoefer, "Generalized dispersion analysis and spurious modes of 2-D and 3-D TLM formulations," *IEEE Trans. Microw. Theory Techn.*, vol. 41, no. 8, pp. 1375–1384, Aug. 1993.

[26] A. Taflove and S. C. Hagness, *Computational Electrodynamics: The Finite-Difference Time-Domain Method* (Artech House antennas and propagation library), 3rd ed. Norwood, MA, USA: Artech House, 2005.

[27] K. S. Kunz and R. J. Luebbers, *The Finite Difference Time Domain Method for Electromagnetics*. Boca Raton, FL, USA: CRC Press, 1993.

[28] J.-M. Jin, *The Finite Element Method in Electromagnetics*. Hoboken, NJ, USA: Wiley, 2015.

[29] R. F. Harrington, *Field Computation by Moment Methods* (IEEE Press Series on Electromagnetic Waves). New York, NY, USA: IEEE Press, 1993.

[30] C. A. Dorao and H. A. Jakobsen, "The quadrature method of moments and its relationship with the method of weighted residuals," *Chem. Eng. Sci.*, vol. 61, no. 23, pp. 7795–7804, Dec. 2006.

[31] W. C. Chew, M. S. Tong, and B. Hu, "Integral equation methods for electromagnetic and elastic waves," *Synth. Lectures Comput. Electromagn.*, vol. 3, no. 1, pp. 1–241, 2008.

[32] M. Taskinen and P. Ylä-Oijala, "Current and charge integral equation formulation," *IEEE Trans. Antennas Propag.*, vol. 54, no. 1, pp. 58–67, Jan. 2006.

[33] S. M. Rao, D. R. Wilton, and A. W. Glisson, "Electromagnetic scattering by surfaces of arbitrary shape," *IEEE Trans. Antennas Propag.*, vol. AP-30, no. 3, pp. 409–418, May 1982.

[34] O. Ergul and L. Gurel, "Investigation of the inaccuracy of the MFIE discretized with the RWG basis functions," in *Proc. IEEE Antennas Propag. Soc. Symp.*, Jun. 2004, pp. 3393–3396.

[35] W. Lei, H. Shao, and J. Hu, "An efficient integral equation model-order reduction method for complex radiation problem," *IEEE Antennas Wireless Propag. Lett.*, vol. 20, no. 7, pp. 1205–1209, Jul. 2021.

[36] S. Amari, J. Bornemann, and R. Vahldieck, "Accurate analysis of scattering from multiple waveguide discontinuities using the coupled-integral equations technique," *J. Electromagn. Waves Appl.*, vol. 10, no. 12, pp. 1623–1644, Jan. 1996.

[37] J.-S. Zhao and W. C. Chew, "Integral equation solution of Maxwell's equations from zero frequency to microwave frequencies," *IEEE Trans. Antennas Propag.*, vol. 48, no. 10, pp. 1635–1645, Oct. 2000.

[38] T. Itoh, "Spectral domain immitance approach for dispersion characteristics of generalized printed transmission lines," *IEEE Trans. Microw. Theory Techn.*, vol. MTT-28, no. 7, pp. 733–736, Jul. 1980.

[39] S. L. Ho, S. Yang, J. M. Machado, and H. C. Wong, "Application of a meshless method in electromagnetics," *IEEE Trans. Magn.*, vol. MAG-37, no. 5, pp. 3198–3202, Sep. 2001.

[40] T. Kaufmann, Y. Yu, C. Engström, Z. Chen, and C. Fumeaux, "Recent developments of the meshless radial point interpolation method for time-domain electromagnetics," *Int. J. Numer. Modelling: Electron. Netw., Devices Fields*, vol. 25, nos. 5–6, pp. 468–489, Sep. 2012.

[41] J. G. Wang and G. R. Liu, "A point interpolation meshless method based on radial basis functions," *Int. J. Numer. Methods Eng.*, vol. 54, no. 11, pp. 1623–1648, 2002.

[42] S. Yang, Z. Chen, Y. Yu, and S. Ponomarenko, "A divergence-free meshless method based on the vector basis function for transient electromagnetic analysis," *IEEE Trans. Microw. Theory Techn.*, vol. 62, no. 7, pp. 1409–1416, Jul. 2014.

[43] Y. Yu and Z. Chen, "Towards the development of an unconditionally stable time-domain meshless method," *IEEE Trans. Microw. Theory Techn.*, vol. 58, no. 3, pp. 578–586, Mar. 2010.

[44] J. Wang, Z. Chen, J. Li, Y. Yu, and J. Liang, "Towards a unifying computational platform with the node-based meshless method," in *IEEE MTT-S Int. Microw. Symp. Dig.*, Jun. 2018, pp. 1017–1020.

[45] H. Jin and R. Vahldieck, "The frequency-domain transmission line matrix method–A new concept," *IEEE Trans. Microw. Theory Techn.*, vol. 40, no. 12, pp. 2207–2218, Dec. 1992.

[46] K. Yee, "Numerical solution of initial boundary value problems involving Maxwell's equations in isotropic media," *IEEE Trans. Antennas Propag.*, vol. AP-14, no. 3, pp. 302–307, May 1966.

[47] S. Akhtarzad and P. Johns, "Solution of 6-component electromagnetic fields in three space dimensions and time by the TLM method," *Electron. Lett.*, vol. 10, no. 25, pp. 535–536, Dec. 1974.

[48] W. J. R. Hoefer, "The transmission-line matrix method-theory and applications," *IEEE Trans. Microw. Theory Techn.*, vol. MTT-33, no. 10, pp. 882–893, Oct. 1985.

[49] P. B. Johns and R. L. Beurle, "Numerical solution of 2-dimensional scattering problems using a transmission-line matrix," *Proc. Inst. Elect. Eng.*, vol. 118, no. 9, pp. 1203–1208, Sep. 1971.

[50] P. B. Johns, "A symmetrical condensed node for the TLM method," *IEEE Trans. Microw. Theory Techn.*, vol. MTT-35, no. 4, pp. 370–377, Apr. 1987.

[51] Z. Chen, "The transmission line matrix (TLM) method and its boundary treatments," M.S. thesis, Dept. Elect. Eng., Univ. Ottawa, Ottawa, ON, Canada, 1992.

[52] M. Krumpholz, C. Huber, and P. Russer, "A field theoretical comparison of FDTD and TLM," *IEEE Trans. Microw. Theory Techn.*, vol. 43, no. 8, pp. 1935–1950, Aug. 1995.

[53] Z. Chen, M. M. Ney, and W. J. R. Hoefer, "A new finite-difference time-domain formulation and its equivalence with the TLM symmetrical condensed node," *IEEE Trans. Microw. Theory Techn.*, vol. 39, no. 12, pp. 2160–2169, Dec. 1991.

[54] J.-F. Lee, R. Lee, and A. Cangellaris, "Time-domain finite-element methods," *IEEE Trans. Antennas Propag.*, vol. 45, no. 3, pp. 430–442, Mar. 1997.

[55] W. H. Reed and T. R. Hill, "Triangular mesh methods for the neutron transport equation," Los Alamos Scientific Lab., Santa Fe, NM, USA, Tech. Rep. LA-UR-73-479, 1973.

[56] B. Cockburn and C.-W. Shu, "TVB runge-kutta local projection discontinuous Galerkin finite element method for conservation laws. II. general framework," *Math. Comput.*, vol. 52, no. 186, pp. 411–435, 1989.

[57] J. Chen and Q. H. Liu, "Discontinuous Galerkin time-domain methods for multiscale electromagnetic simulations: A review," *Proc. IEEE*, vol. 101, no. 2, pp. 242–254, Feb. 2013.

[58] C. L. Bennett and W. L. Weeks, *A Technique for Computing Approximate Electromagnetic Impulse Response of Conducting Bodies*. Purdue Univ., 1968.

[59] S. M. Rao, *Time Domain Electromagnetics*. Amsterdam, The Netherlands: Elsevier, 1999.

[60] S. M. Rao and D. R. Wilton, "Transient scattering by conducting surfaces of arbitrary shape," *IEEE Trans. Antenn. Propag.*, vol. 39, no. 1, pp. 56–61, Jan. 1991.

[61] S. Dodson, S. Walker, and M. Bluck, "Implicitness and stability of time domain integral equation scattering analyses," *Appl. Comput. Electrom. Soc. J.*, vol. 13, no. 3, pp. 291–301, 1998.

[62] B. Shanker, A. A. Ergin, K. Aygun, and E. Michielssen, "Analysis of transient electromagnetic scattering from closed surfaces using a combined field integral equation," *IEEE Trans. Antennas Propag.*, vol. 48, no. 7, pp. 1064–1074, Jul. 2000.

[63] A. E. Yilmaz, J.-M. Jin, and E. Michielssen, "Time domain adaptive integral method for surface integral equations," *IEEE Trans. Antennas Propag.*, vol. 52, no. 10, pp. 2692–2708, Oct. 2004.

[64] E. van't Wout, D. R. van der Heul, H. van der Ven, and C. Vuik, "Design of temporal basis functions for time domain integral equation methods with predefined accuracy and smoothness," *IEEE Trans. Antennas Propag.*, vol. 61, no. 1, pp. 271–280, Jan. 2013.

[65] G. Pisharody and D. S. Weile, "Robust solution of time-domain integral equations using loop-tree decomposition and bandlimited extrapolation," *IEEE Trans. Antennas Propag.*, vol. 53, no. 6, pp. 2089–2098, Jun. 2005.

[66] Y. L. Hu and R. S. Chen, "Analysis of scattering from composite conducting dispersive dielectric objects by time-domain volume-surface integral equation," *IEEE Trans. Antennas Propag.*, vol. 64, no. 5, pp. 1984–1989, May 2016.

[67] G. Pisharody and D. S. Weile, "Electromagnetic scattering from perfect electric conductors using an augmented time-domain integral-equation technique," *Microw. Opt. Technol. Lett.*, vol. 45, no. 1, pp. 26–31, 2005.

[68] K. Sankaran, "Are you using the right tools in computational electromagnetics?" *Eng. Rep.*, vol. 1, no. 3, pp. 1–19, Oct. 2019.

[69] Q. H. Liu, L. Jiang, and W. C. Chew, "Large-scale electromagnetic computation for modeling and applications," *Proc. IEEE*, vol. 101, no. 2, pp. 223–226, Feb. 2013.

[70] W. C. Chew and L. J. Jiang, "Overview of large-scale computing: The past, the present, and the future," *Proc. IEEE*, vol. 101, no. 2, pp. 227–241, Feb. 2013.

[71] M. Yang, B. Wu, H. Gao, and X. Sheng, "A ternary parallelization approach of MLFMA for solving electromagnetic scattering problems with over 10 billion unknowns," *IEEE Trans. Antennas Propag.*, vol. 67, no. 11, pp. 6965–6978, Nov. 2019.

[72] S. Hughey, H. M. Aktulga, M. Vikram, M. Lu, B. Shanker, and E. Michielssen, "Parallel wideband MLFMA for analysis of electrically large, nonuniform, multiscale structures," *IEEE Trans. Antennas Propag.*, vol. 67, no. 2, pp. 1094–1107, Feb. 2019.

[73] S. Omar and D. Jiao, "A linear complexity direct volume integral equation solver for full-wave 3-D circuit extraction in inhomogeneous materials," *IEEE Trans. Microw. Theory Techn.*, vol. 63, no. 3, pp. 897–912, Mar. 2015.

[74] A. Sharshevsky, Y. Brick, and A. Boag, "Direct solution of scattering problems using generalized source integral equations," *IEEE Trans. Antennas Propag.*, vol. 68, no. 7, pp. 5512–5523, Jul. 2020.

[75] H.-T. Meng, B.-L. Nie, S. Wong, C. Macon, and J.-M. Jin, "GPU accelerated finite-element computation for electromagnetic analysis," *IEEE Antennas Propag. Mag.*, vol. 56, no. 2, pp. 39–62, Apr. 2014.

[76] S. Peng and C. F. Wang, "Precorrected-FFT method on graphics processing units," *IEEE Trans. Antennas Propag.*, vol. 61, no. 4, pp. 2099–2107, Apr. 2013.

[77] F.-G. Hu and C.-F. Wang, "Modeling of waveguide structures using DG-FETD method with higher order tetrahedral elements," *IEEE Trans. Microw. Theory Techn.*, vol. 60, no. 7, pp. 2046–2054, Jul. 2012.

[78] Z. Peng, K.-H. Lim, and J.-F. Lee, "Nonconformal domain decomposition methods for solving large multiscale electromagnetic scattering problems," *Proc. IEEE*, vol. 101, no. 2, pp. 298–319, Feb. 2013.

[79] D. Szypulski, G. Fotyga, V. de la Rubia, and M. Mrozowski, "A subspace-splitting moment-matching model-order reduction technique for fast wideband FEM simulations of microwave structures," *IEEE Trans. Microw. Theory Techn.*, vol. 68, no. 8, pp. 3229–3241, Aug. 2020.

[80] J.-M. Jin and S. Yan, "Multiphysics modeling in electromagnetics: Technical challenges and potential solutions," *IEEE Antennas Propag. Mag.*, vol. 61, no. 2, pp. 14–26, Apr. 2019.

[81] H. Van der Vorst, *Iterative Krylov Methods for Large Linear Systems*, Cambridge, U.K.: Cambridge Univ. Press, 2003.

[82] V. P. Nguyen, T. Rabczuk, S. Bordas, and M. Duflot, "Meshless methods: A review and computer implementation aspects," *Math. Comput. Simul.*, vol. 79, no. 3, pp. 763–813, 2008.

[83] M. A. Krasnoselskii, G. M. Vainikko, R. P. Zabreyko, Y. B. Ruticki, and V. V. Stetsenko, *Approximate Solution of Operator Equations*. New York, NY, USA: Springer, 2012.

[84] G. Chen, M. Chen, and Z. Chen, *Approximate Solutions of Operator Equations*, Vol. 9. Singapore: World Scientific, 1997.

[85] S. Mikhlin and K. Smolitskii, *Approximate Methods for Solution of Differential and Integral Equations*. New York, NY, USA: Elsevier; 1967.

[86] Z. Chen and S. Luo, "Generalization of the finite-difference-based time-domain methods using the method of moments," *IEEE Trans. Antennas Propag.*, vol. 54, no. 9, pp. 2515–2524, Sep. 2006.

[87] R. A. Chilton and R. Lee, "Conservative and provably stable FDTD subgridding," *IEEE Trans. Antennas Propag.*, vol. 55, no. 9, pp. 2537–2549, Sep. 2007.

[88] W. Tierens and D. De Zutter, "BOR-FDTD subgridding based on finite element principles," *J. Comput. Phys.*, vol. 230, no. 12, pp. 4519–4535, Jun. 2011.

[89] R. A. Chilton, "H-, P- and T-refinement strategies for the finite difference time-domain (FDTD) method developed via finite-element (FE) principles," Ph.D. dissertation, Dept. Elect. Comput. Eng., Ohio State Univ., Columbus, OH, USA, 2008.

[90] Z. Chen and J. Li, "Unification of numerical methods with the method of weighted residuals and meshless method," in *Proc. IEEE AP-S/URSI*, Singapore, Dec. 2021, pp. 1017–1020.

Zhizhang (David) Chen (Fellow, IEEE) received the B.Eng. degree in radio engineering from Fuzhou University, Fuzhou, Fujian, China, in 1982, the master's degree in radio engineering from Southeast University, Nanjing, China, in 1986, and the Ph.D. degree in electrical engineering from the University of Ottawa, Ottawa, ON, Canada, in 1992.

He was a Natural Sciences and Engineering Research Council (NSERC) Post-Doctoral Fellow with McGill University, Montreal, QC, Canada, in 1993. He is currently with the College of Physics and Information Engineering, Fuzhou University, on leave from the Department of Electrical and Computer Engineering, Dalhousie University, Halifax, NS, Canada, where he is a Professor and the former Head of the Department of Electrical and Computer Engineering. He has been an Adjunct or Visiting Professor with the University of Nottingham, Nottingham, U.K.; École Nationale Supérieure des Télécommunications de Bretagne, Brest, France; Shanghai Jiao Tong University, Shanghai, China; Fuzhou University; Hong Kong University of Science and Technology, Hong Kong; and the University of Electronic Science and Technology of China, Chengdu, China. He has authored and coauthored over 410 journals and conference papers in computational electromagnetics, RF/microwave electronics, antennas, and wireless technologies. He was one of the originators of the unconditionally stable methods that have been highly cited and used. He and his team also developed several nonlinear ultra-wideband receivers and planar wireless power transfer transmitting and receiving structures. His current research interests include time-domain electromagnetic modeling techniques, antennas, wideband wireless communication and sensing systems, and wireless power technology.

Dr. Chen is a Fellow of the Canadian Academy of Engineering and the Engineering Institute of Canada. He received the 2005 Nova Scotia Engineering Award, the 2006 Dalhousie Graduate Teaching Award, the 2007 and 2015 Dalhousie Faculty of Engineering Research Award, the 2013 IEEE Canada Fessenden Medal, and the Dalhousie University Professorship. He was the founding Chair of the joint Signal Processing and Microwave Theory and Techniques Chapter of IEEE Atlantic Canada, the Chair of the IEEE Canada Atlantic Section, and a member of the Board of Directors for IEEE Canada from 2000 to 2001. He has served as a Guest Editor for the IEEE TRANSACTIONS ON MICROWAVE THEORY AND TECHNIQUES, *IEEE Microwave Magazine*, IEEE JOURNAL OF ELECTROMAGNETICS, RF AND MICROWAVE IN MEDICINE AND BIOLOGY, and the *International Journal of Numerical Modeling* (John Wiley) and an Associate Editor for the IEEE JOURNAL ON MULTISCALE AND MULTIPHYSICS COMPUTATIONAL TECHNIQUES. He currently served as a Track Editor for the IEEE TRANSACTIONS ON MICROWAVE THEORY AND TECHNIQUES, a Topic Editor for the IEEE JOURNAL OF MICROWAVES, and an Elected Member of the Ad-Com of IEEE Antennas and Propagation Society.

Chao-Fu Wang (Senior Member, IEEE) received the B.Sc. degree in mathematics from Henan Normal University, Xinxiang, China, in 1985, the M.Sc. degree in applied mathematics from Hunan University, Changsha, Hunan, China, in 1989, and the Ph.D. degree in electrical engineering from the University of Electronic Science and Technology of China, Chengdu, China, in 1995.

From 1987 to 1996, he was a Lecturer and then an Associate Professor with the Nanjing University of Science and Technology, Nanjing, China. From 1996 to 1999, he was a Post-Doctoral Research Fellow with the Center for Computational Electromagnetics, University of Illinois at Urbana–Champaign, Urbana, IL, USA. He came to Singapore in 1999 to join the National University of Singapore, Singapore, became a Principal Research Scientist in 2011, and was appointed as an Associate Professor under courtesy joint appointment in 2018. He has coauthored *Characteristic Modes: Theory and Applications in Antenna Engineering* (Hoboken, NJ: Wiley, 2015). He has published more than 260 journals and conference papers and filed six international patents published under the Patent Cooperation Treaty (PCT) administered by the World Intellectual Property Organization (WIPO) in the area of computational electromagnetics.

Dr. Wang served as the Chairperson for the IEEE Singapore Microwave Theory and Techniques/Antennas and Propagation (MTT/AP) Chapter in 2013. He was a co-recipient of the 2009 Best *Applied Computational Electromagnetics Society (ACES) Journal* Paper Award. He has been actively involved in organizing many conferences, including the General Chair of the 2020 IEEE International Conference on Computational Electromagnetics (ICCEM 2020) and the Special Session and Short Course Chair of the 2021 IEEE International Symposium on Antennas and Propagation and United States National Committee for the International Union of Radio Science (USNC-URSI) Radio Science Meeting (IEEE AP-S/URSI 2021). As a regular reviewer of many international journals, he is currently an Associate Editor of the IEEE TRANSACTIONS ON MICROWAVE THEORY AND TECHNIQUES, IEEE JOURNAL ON MULTISCALE AND MULTIPHYSICS COMPUTATIONAL TECHNIQUES, *International Journal of Numerical Modelling: Electronic Networks, Devices and Fields*, and *Electronics Letters*. As a Guest Editor of the *International Journal of Numerical Modelling: Electronic Networks, Devices and Fields*, he has successfully edited a special issue (volume 33, issue 2, March/April 2020) on advanced solution methods for modeling complex electromagnetic problems.

Wolfgang J. R. Hoefer (Life Fellow, IEEE) received the Dipl.-Ing. degree from RWTH Aachen, Aachen, Germany, in 1965, the Dr.-Ing. degree from the University of Grenoble, Grenoble, France, in 1968, and the Honorary Dr.-Ing. degree from the Technical University of Munich, Munich, Germany, in 2007.

In 1969, he joined the University of Ottawa, Ottawa, ON, Canada, as a Faculty Member, and was the Chair of Electrical Engineering from 1978 to 1981. In 1992, he joined the University of Victoria, Victoria, BC, Canada, as a Professor and the Natural Sciences and Engineering Research Council (NSERC) of Canada Industrial Research Chair, where until 2006, he led the Computational Electromagnetics Research Laboratory (CERL). From 2009 to 2012, he was a Principal Scientist and the Director of the Independent Investigatorship Department, Institute of High-Performance Computing (IHPC), A∗Star, Singapore. Since 2006, he has been a Professor Emeritus with the University of Victoria. Over the past 40 years, he has also held visiting appointments with the University of Grenoble; the University of Rome "Tor Vergata," Rome, Italy; the University of Nice-Sophia Antipolis, Nice, France; the University of Perugia, Perugia, Italy; the University of Munich, Munich, Germany; and the University of Duisburg, Duisburg, Germany; as well as with the Ferdinand Braun Institute, Berlin, Germany; the ETH Zürich, Zürich, Switzerland; AEG-Telefunken, Backnang, Germany; the Communications Research Centre (CRC), Ottawa, ON, Canada; the Institute of High Performance Computing (IHPC) Singapore, Singapore; and the Georgia Institute of Technology, Atlanta, GA, USA. He is the Founder, and was the President of the Faustus Scientific Corporation, Victoria, BC, from 1996 to 2017.

Dr. Hoefer was a Fellow of the Royal Society of Canada in 2003, the Canadian Academy of Engineering in 2009, the German Academy of Science and Engineering (ACATECH), in 2007, the Engineering Institute of Canada in 2016, the Applied Computational Electromagnetics Society in 2020, and the Electromagnetics Academy [Massachusetts Institute of Technology (MIT)], in 1992. He received the Peter B. Johns Prize in 1990, the Applied Computational Electromagnetics Society (ACES) Mainstay Award in 2004, the IEEE Microwave Theory and Techniques Society (IEEE MTT-S) Distinguished Educator Award in 2006, the IEEE Canada McNaughton Gold Medal in 2009, the IEEE MTT-S Microwave Pioneer Award in 2011, the A∗STAR Most Inspiring Mentor Award in 2012, and the IEEE MTT-S Microwave Career Award in 2022. He was the Chair and Co-Chair of the IEEE MTT-15 Technical Committee on Field Theory from 1989 to 2004 and a Distinguished Microwave Lecturer of the IEEE MTT-S from 2005 to 2007. He was an Associate Editor of the IEEE TRANSACTIONS ON MICROWAVE THEORY AND TECHNIQUES from 1998 to 2000. He was the Managing Editor of the *International Journal of Numerical Modelling* from 1988 to 2009.